A Versatile Conducting Interpenetrating Polymer Network for Sensing and Actuation

Chia-Ju Peng, Tien Anh Nguyen, Kätlin Rohtlaid, Cedric Plesse, Shih-Jui Chen, Luc Chassagne, Barthélemy Cagneau

A Versatile Conducting Interpenetrating Polymer Network for Sensing and Actuation

Chia-Ju Peng[1,2], Tien Anh Nguyen[1], Kätlin Rohtlaid[3], Cédric Plesse[3], Shih-Jui Chen[2], Luc Chassagne[1] and Barthélemy Cagneau[1]

***Abstract*— This work deals with a Conducting-Interpenetrating Polymer Network (C-IPN). The C-IPN exhibits very interesting and promising properties which can make it suitable for applications in robotics as a tool to perform tasks in the fields of manipulation, grasping or force measurement. It is known in the literature that such C-IPN may be actuated and bended to interact with other objects. Some of them can also be used as sensors to characterize the interaction. In this paper, we show that actuation and sensing can be performed at the same time. Moreover, we propose analytical models which can be useful for future work to process the C-IPN output and to control them. All results are verified with experimental data.**

I. INTRODUCTION

Gripping and manipulating microscale objects is a critical issue of many applications in micro-assembly [1], micro-robotics [2], [3], microfluidics, optics [4] or biology [5], [6]. In micro-manufacturing, assembling the components precisely is essential and is handled with techniques such as MEMS [7], [8]. Several micro-grippers and driving techniques have been developed, including electrothermal actuators [9], [10], electrostatic actuators [11], electromagnetic actuators [6], [12], piezoelectric actuators [13], [14], [15], shape memory alloys (SMAs) [16], and electronic conducting polymers (ECPs) [17], [18], [19]. For high precision and reliability, the requirement of sensorized micro-grippers increases [20], [21]. Grippers with embedded sensors to monitor the gripping force are required to manipulate the objects without any damage. However, the available workspace for additional sensors is limited. Integrating sensors and actuators on the same electrode or using actuators with intrinsic sensing capability can save the volume of the final product. Conducting interpenetrating polymer networks (C-IPNs) appear as a potential solution, to design compact grippers that can sense and actuate at the same time with only two wires connected.

C-IPN is a flexible tri-layer structure which comprises two conducting polymer electrodes on each face of the electrolyte membrane. Electronic conducting polymer (ECP) are reactive materials and can be electrochemically oxidized or reduced, while ions exclusion or inclusion from the electrolyte for electroneutrality contributes to volume change of the polymer [22], [23]. The related deformation caused by reversible redox reaction makes ECP popular in the family of electroactive polymers (EAPs), attracting wide attention for actuating application [24]. In recent years, researches of ECP actuators using poly(3,4-ethylenedioxythiophene) (PEDOT) [25], [26] or polypyrrole (PPy) [27], [28] have been proposed. Among them, tri-layer devices consisting of two ECP electrodes and an interjacent solid polymer electrolyte (SPE) as an ionic reservoir can operate in open-air [29], [30]. Moreover, C-IPNs with ECP/SPE/ECP layers have been described. This architecture presents several advantages such as cyclability, good performances, fast response and compact size [31].

In this study, we present a C-IPN that may act both as an actuator and as a sensor, having great potential to be a micro-gripper that actuates and senses the contact at the same time without additional sensor. When electric potential difference is applied between the two electrodes, the ECP electrodes are deformed in opposite direction and bend the conducting C-IPN according to the redox reaction. On the other hand, when the C-IPN is bent by a mechanical stimulus, an electric potential can be measured between the two electrodes due to mechanically induced ion motion between them [32]. The dimensions of C-IPN in this study are in millimeters (for the length and the width) while the thickness is a few hundreds of micrometers. Experimental data are provided but not limited to this scale.

In section II, we briefly present the fabrication process of the C-IPN. More details can be found in [33]. The experimental setup is also presented. In section III, the C-IPN is used as a sensor and experimental results are presented as well as a model. In section IV, a model is proposed for the actuator and we show that contact detection is enabled while actuating. Finally, in section V, a conclusion is drawn and future work is discussed.

II. C-IPN FABRICATION PROCESS AND EXPERIMENTAL SETUP

A. Conducting C-IPN Synthesis

The electroactive material is prepared according to a detailed procedure described elsewhere [33]. The conducting C-IPNs are composed of two ECP electrodes interpenetrated in both faces of a membrane acting as an electrolyte reservoir. The presence of these ions is necessary to make these materials electroactive as actuators and as sensors.

[1]are with Université de Versailles, UVSQ/LISV, 78140 Vélizy, France barthelemy.cagneau@uvsq.fr

[2]are with National central University, Department of Mechanical Engineering, Taoyuan, Taiwan raychen@cc.ncu.edu.tw

[3]are with Université de Cergy, LPPI / I-MAT, Cergy-Pontoise, France cedric.plesse@u-cergy.fr

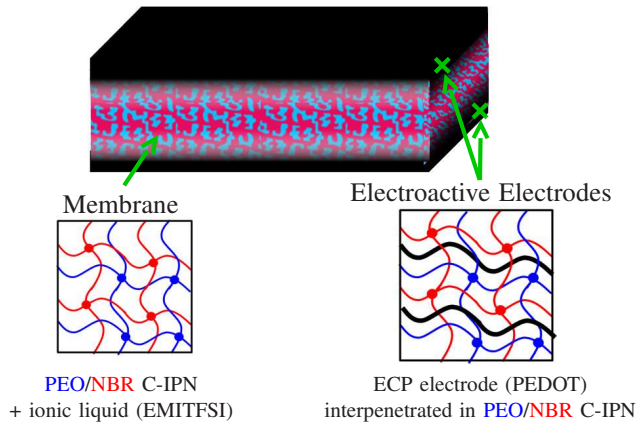

Fig. 1: Schematic representation of the structure and composition of conducting C-IPN used as actuators or/and as sensors

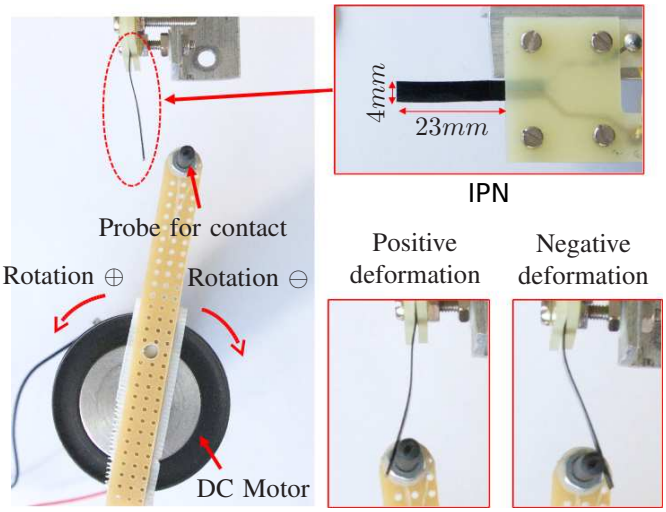

Fig. 2: The C-IPN is actuated with a power supply and disturbances may be applied with a probe connected to a DC motor.

The interpenetrated ECP electrodes, presented in figure 1 are made of poly(3,4-ethylenedioxythiophene) (PEDOT). The membrane is synthesized with a C-IPN architecture with two interpenetrated networks: a poly(ethylene oxide) network (PEO) insuring ionic conductivity through the membrane and a high molecular weight Nitrile Butadiene Rubber (NBR) insuring the mechanical robustness of the final device. After synthesis of the pseudo-trilayer material, the chosen electrolyte, the ionic liquid 1-ethyl-3-methyl-imidazolium bis(trifluoromethylsulfonyl)imide (EMITFSI) is incorporated through a swelling step.

B. Experimental Setup

The experimental setup is represented in figure 2. It consists of 2 distinct parts. The first one is the C-IPN itself with a rectangular shape ($23mm$ in length, $4mm$ in width and a thickness of $250\mu m$). It is actuated with an external power supply.

The second part of the experimental setup is a DC motor which can be actuated and controlled to disturb the C-IPN. A rigid probe may be thus in contact with the C-IPN on its two sides.

III. SENSOR MODE

In this section, we are focused on the sensing capabilities of the C-IPN. Figure 3 briefly describes the schematic used to interact with the C-IPN. The switch may be placed in position 1 to actuate and to bend the C-IPN and in position 2 for sensing purposes. The terms *sensor mode* and *actuator mode* are used hereafter.

A. Electronics Design

In figure 3, U_p is the C-IPN voltage and U_g is the voltage provided by a signal generator. A resistor R may be tuned to adapt the current consumption as well as the dynamical behaviour of the C-IPN.

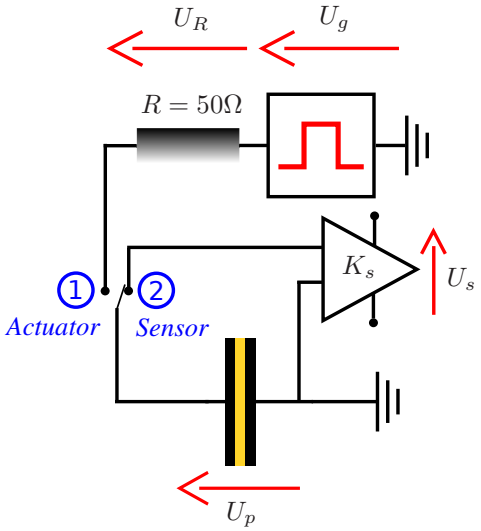

Fig. 3: Illustration of the 2 modes used with the C-IPN.

After first experiments, we can notice that, in sensor mode, U_p is only of a few hundreds of microvolts. It is thus necessary to magnify the signal to perform the acquisition. To solve this problem, an analog amplifier circuit with a tunable gain is proposed in figure 4.

Equation 1 describes the relationship between the input U_p and the output U_s:

$$U_s(t) = K_s\ U_p(t) \tag{1}$$

The circuit of signal conditioning consists of three successive levels of amplification. To decrease electronic noise, the board uses low-noise operational amplifiers of Analog Device OP27. The board has two levels of non-inverting amplifier tuned with a gain of 11. The intermediate level is a differential amplifier with a gain of 10. It allows the compensation for the offset voltage of the transducer that

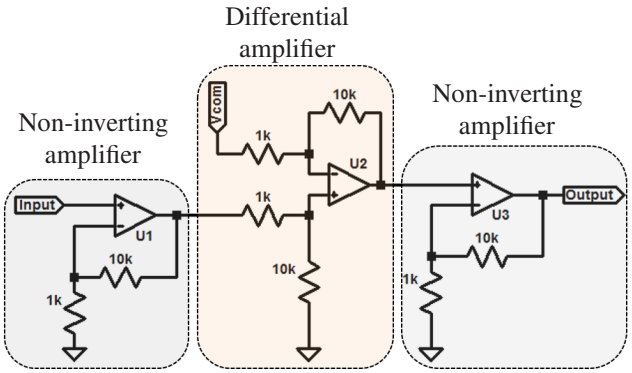

Fig. 4: Electric diagram of the amplifier board. The gain may be tuned and is set to $K_s = 1210$ for experiments

may occur due, for example, to residual deformations. As a consequence, the signal is amplified with a total gain $K_s = 1210$.

B. Experimental Results

We use the DC motor described in section II-B to create passive deformations. The C-IPN is submitted to periodic deformations because of the constant velocity of the motor. After 2 cycles, an opposite voltage is applied to the motor.

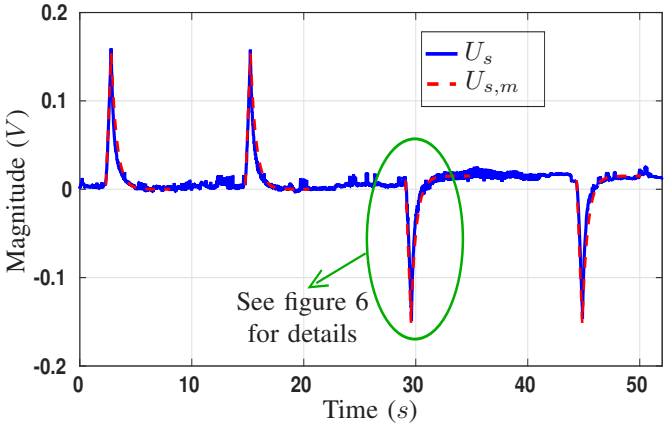

Fig. 5: Amplified sensor output with periodic disturbances. U_s is modeled with $U_{s,m}$

Figure 5 clearly presents four cycles which correspond to 4 disturbances applied to the C-IPN. According to equation 1, U_s is measured and plotted. The amplitude of U_s is about $\pm 0.15V$. This sensitivity is high enough to detect the contact while a deformation occurs.
For each disturbance cycle, 2 different phases are observed:

- The C-IPN seems to be first linearly deformed. This phase happens when the probe is in contact with the C-IPN. It is bended until the contact is broken.
- The voltage U_s is secondly decreasing with an exponential shape. This phase happens when the C-IPN is relaxing to its initial state.

To validate these observations, we have derived an analytical model $U_{s,m}$ for the two observed phases. The proposed model is such that:

$$U_{s,m}(t) = K_s(t - t_0), \text{ for } 0 \leq t \leq t_1 \quad (2)$$

$$U_{s,m}(t) = A_s \exp^{-(t-t_1)/\tau_s} + B_s, \text{ for } t > t_1 \quad (3)$$

$P_s = \{A_s, K_s, \tau_s, B_s\}$ is a set of parameters that we need to identify with experimental data. t_1 corresponds to the time when the contact is broken. t_0 is only a time offset to shift the model with respect to the time t. To identify P_s, we have used the third disturbance cycle in figure 5.

In figure 6, the model $U_{s,m}$ is matching experimental data U_s.

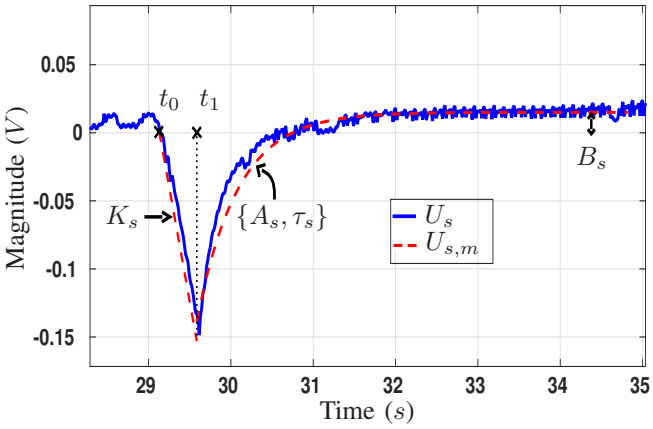

Fig. 6: Zoom on the third cycle

The parameters that we have identified are:

$$\{K_s, A_s, \tau_s, B_s\} = \{-0.32V.s^{-1}, 0.16V, 0.5s, 0.02V\} \quad (4)$$

It is important to notice that the experiments are reproducible. For the fourth cycle in 5, the set P is the same. When switching to the so-called positive deformations, the signs of A_s and K_s have been changed to match the sign of U_s. However, for these first two cycles, $B_s = 0V$. It seems that the two electrodes (the two sides) of the C-IPN are not symmetric. That would explain the different values of B_s depending on the deformations.

To summarize, the amplifier circuit is well suited to detect the deformations that occur on the C-IPN. The electronic board amplifies the C-IPN voltage U_p with a gain $K_s = 1210$. However, the amplitudes of negative and positive impulses are not totally identical because of possible asymmetry of electrodes rising from the synthesis. This could explain the asymmetric behaviour of the two electrodes. The error induced by the lack of symmetry is compensated with the B_s term in the model (see equation 3).

IV. ACTUATOR MODE

In this section, we are focused on the capabilities of the C-IPN to be used as an actuator. As illustrated in figure 3, the switch is positioned to actuate the C-IPN.
In section III, we have shown that the sensor mode is suitable

to detect a contact and measure the variations of the forces applied to it. However, the main interest of C-IPN should be to actuate and to sense at the same time.

A. Actuator Modeling

According to figure 3, U_g is used to actuate the C-IPN. U_g is a square signal with following characterisics:

- Frequency: $f_g = 0.1Hz$
- Magnitude: $M_g = \pm 2V$

At each time, we have also verified that equation 5 is satisfied:

$$\forall t,\ U_g(t) = U_R(t) + U_p(t) \tag{5}$$

In figure 7, U_g and U_p are plotted as functions of time t.

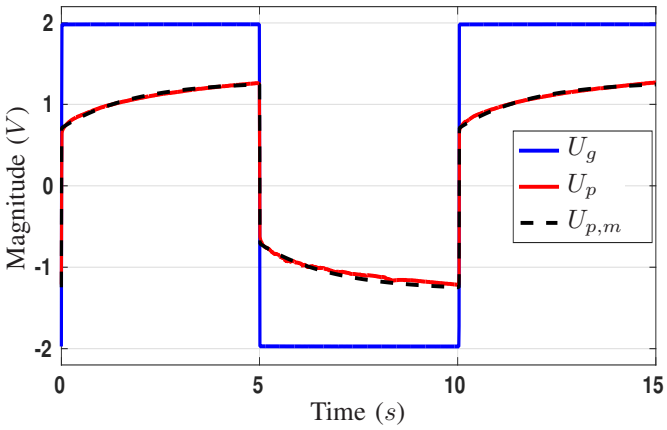

Fig. 7: The C-IPN is actuated with U_g. U_p is measured and modeled with $U_{p,m}$

While the C-IPN is actuated, a peak value around $200mA$ is observed for the current when U_g value is switched. For this experiment, the maximum angle of deformation is $\delta_{max} = \pm 10°$ depending on the sign of U_g.

One of our concern is to derive a model of the actuator which can be used to understand the C-IPN behaviour. According to figure 7, it seems that the shape of U_p is exponential and we have proposed to derive a model $U_{p,m}$ of U_m as:

$$U_{p,m} = \pm \left(A_p * \exp(-(t - t_0)/\tau_p) + B_p\right) \tag{6}$$

The parameters $A_p = 0.57V$, $B_p = 1.28V$ and $\tau_p = 1.80s$ have been identified. The signs of U_p and $U_{p,m}$ only depend on the sign of U_g.

B. Experimental Results

In this section, we want to evaluate the capabilities of the C-IPN to actuate and to sense at the same time. The C-IPN is actuated as described in section IV-A with U_g. We also apply a periodic disturbance on the polymer with the DC motor presented in section II-B. The velocity of the motor is set to a constant velocity so that the frequency f_d of the disturbance is $f_d = 0.5Hz$.
The results are presented in figure 8.

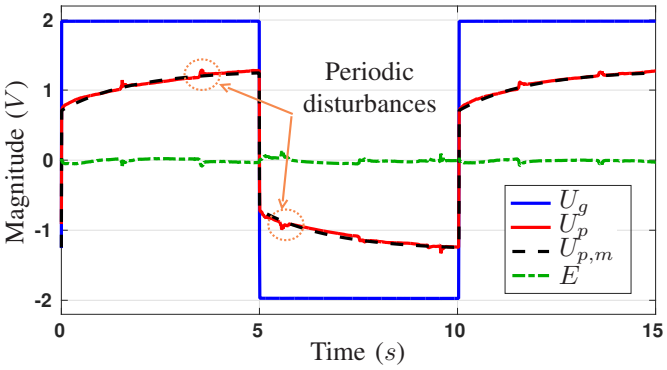

Fig. 8: Periodic disturbances, with a frequency f_d, are applied to the C-IPN while it is actuated

Results are plotted as functions of time. To emphasize these results, the difference E between the C-IPN voltage U_p and its model $U_{p,m}$ is plotted according to equation 7

$$E(t) = U_{p,m}(t) - U_p(t) \tag{7}$$

E represents the component of U_p that corresponds to the disturbance.

The first thing that we can notice is that the model $U_{p,m}$ is still valid for this new experiment. The experiments are indeed reproducible when the same C-IPN is used. The set of parameters needs to be adjusted when the dimensions are changed. The second noticeable thing is that we are able to detect the disturbances applied to the C-IPN while measuring U_p. All disturbances applied to the C-IPN appear on the plot for 15 seconds. It clearly illustrates that we enable actuation and contact detection at the same time on the same electrodes.

In future work, it should be interesting to quantify the deformations and provide the user with better information concerning the contact between the polymer and its environment. That would make the C-IPN suitable for manipulation. In order to improve the setup, it is however required to adapt the electronic board to amplify the signal component that corresponds to the deformation due to the disturbance.

V. CONCLUSION AND FUTURE WORK

In this paper, we have demonstrated the sensing and actuating capabilities of the C-IPN. A remarkable result is that the electronic design and the experimental setup allow to sense and actuate at the same time. However, only binary information like contact/non-contact can be retrieved with this prototype. In future work, we plan to amplify the signal presented in figure 8 to extract precise information about the contact. It will be necessary to process the signal since it contains two components. The first one relates to the contact with a level of a few millivolts. The second one may be of a few volts to actuate the C-IPN.

We are also interested in manipulation at microscales and have developed a C-IPN suitable for this scale. In future work, we hope to demonstrate that similar results can be

achieved at microscale. One of the main advantage is that the shape of the C-IPN can be freely designed. We can thus expect to use these polymers as micro-grippers to perform manipulation tasks.

ACKNOWLEDGMENT

This work is made possible with the support of the French National Research Agency (ANR) and the project MicroTIP.

REFERENCES

[1] J. Agnus, N. Chaillet, C. Clévy, S. Dembélé, M. Gauthier, Y. Haddab, G. J. Laurent, P. Lutz, N. Piat, and M. Rakotondrabe, "Robotic microassembly and micromanipulation at femto-st." *Journal of Micro-Bio Robotics*, vol. 8, no. 2, pp. 91–106, apr 2013.

[2] K. Mølhave, T. Wich, A. Kortschack, and P. Bøggild, "Pick-and-place nanomanipulation using microfabricated grippers," *Nanotechnology*, vol. 17, no. 10, p. 2434, 2006.

[3] M. Gauthier, C. Clévy, D. Hériban, and P. Kallio, "Industrial tools for micromanipulation," in *Micro- and Nanomanipulation Tools*, Y. Sun and Xinyu, Eds. John Wiley and Sons, 2015, ch. 15, pp. 1–25.

[4] X. Shi, W. Chen, J. Zhang, and W. Chen, "Design, modeling, and simulation of a 2-dof microgripper for grasping and rotating of optical fibers," in *2013 IEEE/ASME International Conference on Advanced Intelligent Mechatronics*, July 2013, pp. 1597–1602.

[5] K. Han, S. H. Lee, W. Moon, J. S. Park, and C. W. Moon, "Design and fabrication of the micro-gripper for manipulating the cell," *Integrated Ferroelectrics*, vol. 89, pp. 77–86, 2007.

[6] T. R. Ger, H. T. Huang, W. Y. Chen, and M. F. Lai, "Magnetically-controllable zigzag structures as cell microgripper," *Lab on a Chip*, vol. 13, no. 12, pp. 2364–2369, 2013.

[7] V. Seidemann, S. Butefisch, and S. Buttgenbach, "Fabrication and investigation of in-plane compliant su8 structures for mems and their application to micro valves and micro grippers," *Sensors and Actuators a-Physical*, vol. 97-8, pp. 457–461, 2002.

[8] J. Cecil, D. Vasquez, and D. Powell, "A review of gripping and manipulation techniques for micro-assembly applications," *International Journal of Production Research*, vol. 43, no. 4, pp. 819–828, 2005.

[9] M. Rakotondrabe and I. A. Ivan, "Development and force/position control of a new hybrid thermo-piezoelectric microgripper dedicated to micromanipulation tasks," *Ieee Transactions on Automation Science and Engineering*, vol. 8, no. 4, pp. 824–834, 2011.

[10] K. Carlson, K. N. Andersen, V. Eichhorn, D. H. Petersen, I. Bu, K. Teo, W. Milne, S. Fatikow *et al.*, "A carbon nanofibre scanning probe assembled using an electrothermal microgripper," *Nanotechnology*, vol. 18, no. 34, p. 345501, 2007.

[11] O. Millet, P. Bernardoni, S. Regnier, P. Bidaud, E. Tsitsiris, D. Collard, and L. Buchaillot, "Electrostatic actuated micro gripper using an amplification mechanism," *Sensors and Actuators a-Physical*, vol. 114, no. 2-3, pp. 371–378, 2004.

[12] A. J. Sanchez-Salmeron, R. Lopez-Tarazon, R. Guzman-Diana, and C. Ricolfe-Viala, "Recent development in micro-handling systems for micro-manufacturing," *Journal of Materials Processing Technology*, vol. 167, no. 2-3, pp. 499–507, 2005.

[13] S. K. Nah and Z. W. Zhong, "A microgripper using piezoelectric actuation for micro-object manipulation," *Sensors and Actuators a-Physical*, vol. 133, no. 1, pp. 218–224, 2007.

[14] R. Elfrink, T. Kamel, M. Goedbloed, S. Matova, D. Hohlfeld, Y. Van Andel, and R. Van Schaijk, "Vibration energy harvesting with aluminum nitride-based piezoelectric devices," *Journal of Micromechanics and Microengineering*, vol. 19, no. 9, p. 094005, 2009.

[15] A. M. El-Sayed, A. Abo-Ismail, M. T. El-Melegy, N. A. Hamzaid, and N. A. Abu Osman, "Development of a micro-gripper using piezoelectric bimorphs," *Sensors*, vol. 13, no. 5, pp. 5826–5840, 2013.

[16] M. Mertmann and E. Hornbogen, "Grippers for the micro assembly containing shape memory actuators and sensors," *Journal De Physique Iv*, vol. 7, no. C5, pp. 621–626, 1997.

[17] M. Y. Benslimane, H. E. Kiil, and M. J. Tryson, "Dielectric electro-active polymer push actuators: performance and challenges," *Polymer International*, vol. 59, no. 3, pp. 415–421, 2010.

[18] A. Maziz, C. Plesse, C. Soyer, C. Chevrot, D. Teyssie, E. Cattan, and F. Vidal, "Demonstrating khz frequency actuation for conducting polymer microactuators," *Advanced Functional Materials*, vol. 24, no. 30, pp. 4851–4859, 2014.

[19] S. Bhattacharya, B. Bepari, and S. Bhaumik, "Ipmc-actuated compliant mechanism-based multifunctional multifinger microgripper," *Mechanics Based Design of Structures and Machines*, vol. 42, no. 3, pp. 312–325, 2014.

[20] J. Park and W. Moon, "A hybrid-type micro-gripper with an integrated force sensor," *Microsystem Technologies-Micro-and Nanosystems-Information Storage and Processing Systems*, vol. 9, no. 8, pp. 511–519, 2003.

[21] D. H. Kim, B. Kim, and H. Kang, "Development of a piezoelectric polymer-based sensorized microgripper for microassembly and micromanipulation," *Microsystem Technologies-Micro-and Nanosystems-Information Storage and Processing Systems*, vol. 10, no. 4, pp. 275–280, 2004.

[22] R. H. Baughman, "Conducting polymer artificial muscles," *Synthetic Metals*, vol. 78, no. 3, pp. 339–353, 1996.

[23] E. Smela, "Conjugated polymer actuators for biomedical applications," *Advanced materials*, vol. 15, no. 6, pp. 481–494, 2003.

[24] T. Mirfakhrai, J. D. W. Madden, and R. H. Baughman, "Polymer artificial muscles," *Materials Today*, vol. 10, no. 4, pp. 30–38, 2007.

[25] A. Khaldi, C. Plesse, C. Soyer, E. Cattan, F. Vidal, C. Legrand, and D. Teyssie, "Conducting interpenetrating polymer network sized to fabricate microactuators," *Applied Physics Letters*, vol. 98, no. 16, p. 3, 2011.

[26] S. Taccola, F. Greco, B. Mazzolai, V. Mattoli, and E. W. H. Jager, "Thin film free-standing pedot:pss/su8 bilayer microactuators," *Journal of Micromechanics and Microengineering*, vol. 23, no. 11, 2013.

[27] E. W. Jager, N. Masurkar, N. F. Nworah, B. Gaihre, G. Alici, and G. M. Spinks, "Patterning and electrical interfacing of individually controllable conducting polymer microactuators," *Sensors and Actuators B: Chemical*, vol. 183, pp. 283–289, 2013.

[28] D. Melling, S. A. Wilson, and E. W. H. Jager, "Controlling the electro-mechanical performance of polypyrrole through 3-and 3,4-methyl substituted copolymers," *Rsc Advances*, vol. 5, no. 102, pp. 84 153–84 163, 2015.

[29] D. Aradilla, M. M. Perez-Madrigal, F. Estrany, D. Azambuja, J. I. Iribarren, and C. Aleman, "Nanometric ultracapacitors fabricated using multilayer of conducting polymers on self-assembled octanethiol monolayers," *Organic Electronics*, vol. 14, no. 6, pp. 1483–1495, 2013.

[30] N. Festin, C. Plesse, P. Pirim, C. Chevrot, and F. Vidal, "Electro-active interpenetrating polymer networks actuators and strain sensors: Fabrication, position control and sensing properties," *Sensors and Actuators B-Chemical*, vol. 193, pp. 82–88, 2014.

[31] C. Plesse, A. Khaldi, Q. Wang, E. Cattan, D. Teyssie, C. Chevrot, and F. Vidal, "Polyethylene oxide-polytetrahydrofurane-pedot conducting interpenetrating polymer networks for high speed actuators," *Smart Materials and Structures*, vol. 20, no. 12, 2011.

[32] Y. Wu, G. Alici, J. Madden, G. Spinks, and G. Wallace, "Soft mechanical sensors through reverse actuation in polypyrrole," *Advanced Functional Materials*, vol. 17, no. 16, pp. 3216–3222, 2007.

[33] N. Festin, A. Maziz, C. Plesse, D. Teyssi, C. Chevrot, and F. Vidal, "Robust solid polymer electrolyte for conducting ipn actuators," *Smart Materials and Structures*, vol. 22, no. 10, p. 104005, 2013.